ELSEVIER

25 April 1997

Chemical Physics Letters 269 (1997) 107–116

CHEMICAL PHYSICS LETTERS

A computational study of the reactions of atomic hydrogen with fluoromethanes: kinetics and product channels

R.J. Berry [a], C.J. Ehlers [a], D.R. Burgess Jr. [b], M.R. Zachariah [b], P. Marshall [a,c]

[a] *Center for Computational Modeling of Nonstructural Materials, Wright Laboratory, Materials Directorate, Wright-Patterson AFB, OH 45433, USA*

[b] *Chemical Science and Technology Laboratory, National Institute of Standards and Technology, Gaithersburg, MD 20899, USA*

[c] *Department of Chemistry, University of North Texas, Denton, TX 76203, USA*

Received 29 August 1996; in final form 11 February 1997

Abstract

Transition states for the H-abstraction, F-abstraction and substitution pathways of the reaction of H with fluoromethanes were characterized at the HF and MP2(FU) levels of theory with the 6-31G(d) basis set. The reaction barrier heights for these pathways were obtained from single point energy calculations using the Gaussian-2 and BAC-MP4 methods. These results were employed to calculate rate constants via transition state theory. The computed rate constants are in good accord with available experimental data, and are discussed in the context of the differing flame suppression chemistries of CH_3F, CH_2F_2, CHF_3 and CF_4.

1. Introduction

Kinetic data for the reactions of H atoms with fluorinated methanes are needed to model the combustion chemistry of fluorine-containing compounds. This topic has received recent attention through efforts to understand the flame suppression activity of halons such as CF_3Br and potential substitutes [1–5]. For typical hydrocarbon flames (achieving temperatures in the range 1600–2200 K) numerical simulations of the decomposition of the fluoromethanes in conjunction with flame speed measurements [6] indicate that a major destruction pathway for the fluoromethanes is through abstraction of H from the fluoromethanes by H atoms in the flame. This pathway competes with the other major destruction pathways, including H-atom abstraction by OH radicals and unimolecular decomposition (HF elimination). The relative importance of each pathway depends upon the fuel, stoichiometry (fuel/oxidizer ratio), inhibitor, and inhibitor concentration. For example, for stoichiometric methane–air flames at high inhibitor concentrations, the relative amounts of fluoromethane destroyed via the reaction with H atoms, unimolecular decomposition, and via reaction with OH radicals are 6 : 3 : 1 and 4 : 3 : 3 for CHF_3 nyand CH_2F_2, respectively. By contrast to the process

$$H + CH_4 \rightarrow CH_3 + H_2, \quad (1)$$

the experimental kinetic data base for H-atom reactions with fluorinated molecules is sparse and sometimes contradictory. For example, three pathways for

PII S0009-2614(97)00248-0

attack by H on CH_3F have been discussed in the literature [7]; abstraction of F, abstraction of H, and substitution

$$H + CH_3F \rightarrow CH_3 + HF, \quad \Delta H_{298} = -111 \text{ kJ mol}^{-1}; \qquad (2f)$$

$$\rightarrow CH_2F + H_2, \quad \Delta H_{298} = -16 \text{ kJ mol}^{-1}; \qquad (2h)$$

$$\rightarrow CH_4 + F, \quad \Delta H_{298} = -12 \text{ kJ mol}^{-1}. \qquad (2s)$$

The exothermicities [8,9] demonstrate that all these channels are thermochemically reasonable. The dominance of the F-abstraction channel has been generally assumed based on experimental work by Westenberg and deHaas [7]. Recent BAC-MP4 results of Westmoreland et al. [5] indicate that H-abstraction is the most important pathway. At the same time, experimental estimates of the total rate constant, k_2, differ by more than two orders of magnitude at 600 K, where different measurement techniques overlap [7].

Here the results of high-level ab initio calculations are presented for abstraction and substitution pathways for the series $H + CH_{4-x}F_x$ ($x = 0$–4), i.e. reactions (1), (2) and the reactions,

$$H + CH_2F_2 \rightarrow \text{products}, \qquad (3)$$

$$H + CHF_3 \rightarrow \text{products}, \qquad (4)$$

$$H + CF_4 \rightarrow \text{products}. \qquad (5)$$

There are limited data for many of these reactions. Consequently one aim of this work is to develop rate expressions suitable for use in combustion modeling.

It is known that Gaussian-2 theory [10], which approximates QCISD(T)/6-311 + G(3df,2p), yields results that are in accord with experimental atomization energies for a test set of bound molecules with an average absolute deviation of 5 kJ mol^{-1}. This test set did not include fluorocarbon molecules. Similarly, the BAC-MP4 method has been shown [11] to predict enthalpies of formation for fluorinated hydrocarbons to within 10 kJ mol^{-1}. In this study, we estimate barrier heights using the G2 and BAC-MP4 methods to see whether similar degrees of accuracy hold for various transition states. These results are employed in transition state theory calculations to yield rate expressions and product branching ratios for reactions (1)–(5). The implications for models of flame suppression by fluorinated agents are also discussed.

2. Theoretical methods

The ab initio calculations were conducted on Cray-YMP, HP-PARisc, SGI-Power Challenge and SUN-SVR4 computers [1] using the GAUSSIAN 92 code [12]. The geometries of the reactants, transition state (TS) and products for each reaction were initially optimized at the HF level of theory using the 6-31G(d) basis set. Next, these optimized geometries were further refined at the MP2(FU) level with the 6-31G(d) basis set. Finally, these MP2 optimized geometries were utilized to obtain approximate QCISD(T)/6-311 + G(3df,2p) energies via the G2(MP2) and G2(ZPE = MP2) [10] protocols. For the "G2 test" species, the G2(MP2) variation has been shown to provide accurate atomization energies without the use of the computationally expensive MP4/6-311G(2df,p) energy evaluation. On the other extreme, the G2(ZPE = MP2) procedure requires this expensive step as well as MP2 vibrational frequencies instead of HF frequencies. For the BAC-MP4 calculations, MP4/6-31G(d,p) single point energies were calculated using HF/6-31G(d) optimized geometries followed by empirical bond additivity corrections (BACs).

Vibrational frequencies were computed at the HF and MP2 geometries in order to verify that the optimizations resulted in true minima (with no complex frequencies) or transition states (with only one complex frequency corresponding to motion along the reaction coordinate). The vibrational frequencies (scaled by a standard scale factor of 0.8929 for HF and 0.9646 for MP2 [10]) were also used to compute the zero-point energy (ZPE) correction for the G2(MP2) and G2(ZPE = MP2) energies.

[1] Certain commercial equipment, instuments, or materials are identified in this paper in order to specify the experimental procedure adequately. In no case does such identification imply recommendation or endorsement by the National Institute of Standards and Technology, nor does it imply that the materials or equipment are necessarily the best available for the purpose.

The bimolecular rate constant k for each pathway was obtained from canonical transition state theory (TST) calculations as implemented within the POLYRATE 6.5 program [13]

$$k_{TST} = \Gamma \frac{k_B T}{h} \frac{Q_{TS^{\ddagger}}}{Q_H Q_{CH_{4-x}F_x}} \exp\left(-\frac{E_0^{\ddagger}}{RT}\right), \qquad (6)$$

where Γ represents a correction factor for quantum mechanical tunneling derived at the zero-curvature level and is $\geqslant 1$ [14]. The partition functions include rotational symmetry numbers. $E_0^{\ddagger}$ is the energy difference between reactants and TS including ZPE, i.e. the enthalpy difference at 0 K. The rate constants based on the BAC-MP4 calculations were evaluated from the partition functions, Q, without considering tunneling. Consequently, at low temperatures (300–800 K) these values will significantly underpredict the rates of reaction. However, at typical flame temperatures (1600–2200 K), this difference will be small. The G2 based results do include a tunneling contribution.

3. Results and discussion

The optimized geometrical parameters associated with the reaction coordinate of the TSs for the hydrogen abstraction, fluorine abstraction and substitution channels are illustrated in Fig. 1. The components of their G2(MP2) and G2(ZPE = MP2) energies are listed in Table 1 along with the MP4/6-31G(d,p)//HF/6-31G(d) energy utilized in the BAC-MP4 calculation. For the reactants and products the optimized geometries, component energies and enthalpies of formation are available elsewhere [10,15–17]. Table 2 lists the computed barrier heights for the H-abstraction, F-abstraction and substitution channels.

For the H-abstraction reactions, TS properties have been analyzed previously only for the reaction $H + CH_4 \rightarrow CH_3 + H_2$. Some representative earlier values [18–23] of the barrier, $E_0^{\ddagger}$, are compared in Table 2. The BAC-MP4 and G2 values calculated here are seen to be in good accord with other ab

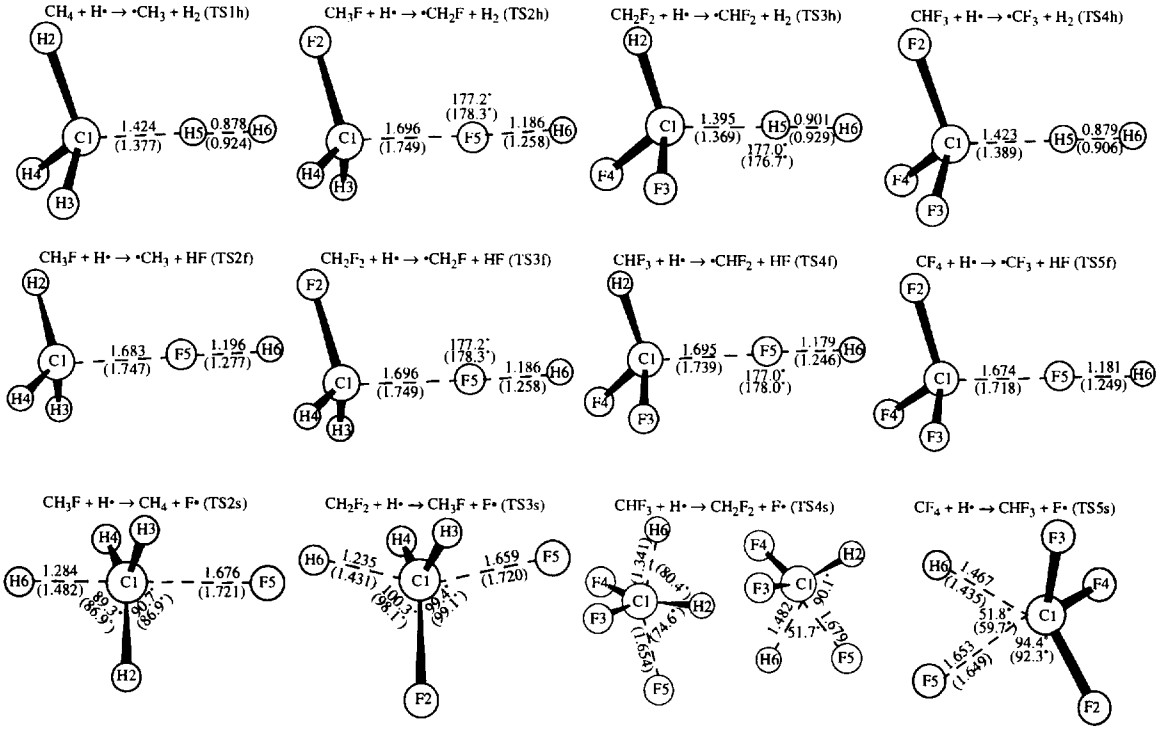

Fig. 1. Optimized MP2(HF in parentheses)/6-31G(d) transition state geometries for fluoromethane hydrogen abstraction (TS1h–TS4h); fluorine abstraction (TS2f–TS5f); and fluorine substitution (TS2s–TS5s) reactions.

Table 1
Calculated BAC-MP4, G2(MP2) and G2(ZPE = MP2) energy components and ground state energies [a] for the transition states of H + fluoromethanes

Species	ZPE(scaled)		BAC-MP4 [b]		E [c]	Δ(QCI)	G2(MP2) [d]		G2(ZPE = MP2) [e]			
	(HF)	(MP2)	E[MP4]	E_0[MP4]			Δ(MP2)	E_0	$\Delta(+)$	Δ(2df)	Δ	E_0
TS1h	40.19	42.69	−40.85584	−40.81083	−40.87725	−2.94	−26.50	−40.88669	−0.56	−18.71	−8.55	−40.88679
TS2h	35.08	36.80	−139.85650	−139.81721	−139.94181	−1.88	−86.38	−140.03017	−8.93	−69.76	−11.74	−140.03474
TS2f	36.48	38.87	−139.82022	−139.77937	−139.90695	−4.51	−91.14	−140.00132	−14.91	−68.54	−11.90	−140.00538
TS2s	38.33	40.59	−139.81626	−139.77333	−139.90625	−4.91	−92.09	−140.00011	−13.49	−70.99	−12.41	−140.00488
TS3h	28.94	30.04	−238.87775	−238.84534	−239.02565	−0.30	−144.19	−239.19140	−14.21	−121.91	−15.16	−239.20057
TS3f	31.00	32.76	−238.83202	−238.79730	−238.98063	−3.41	−149.08	−239.15231	−21.26	−119.89	−15.11	−239.16092
TS3s	32.45	34.28	−238.81495	−238.77861	−238.96729	−3.85	−149.32	−239.13820	−18.72	−122.00	−16.28	−239.14725
TS4h	21.73	22.50	−337.90810	−337.88377	−338.11683	1.50	−200.93	−338.35972	−17.69	−174.94	−18.73	−338.37353
TS4f	24.48	25.66	−337.85873	−337.83131	−338.06732	−2.25	−205.62	−338.31591	−25.21	−172.58	−18.28	−338.32933
TS4s	25.59	27.28	−337.83077	−337.80212	−338.04362	2.14	−204.17	−338.28525	−21.11	−174.11	−19.33	−338.29810
TS5f	17.08	17.81	−436.88699	−436.86786	−437.15510	−0.94	−261.05	−437.48019	−27.38	−226.04	−21.60	−437.49855
TS5s	18.92	18.83	−436.85880	−436.83761	−437.12865	4.11	−260.32	−437.44613	−23.55	−227.76	−22.73	−437.46505

[a] Energies in au and energy components in 10^{-3} au.

[b] Energies computed with the 6-31G(d, p) basis set. E_0[MP4] = E[MP4] + ZPE (HF, unscaled).

[c] Energies computed at the MP4/6-311G(d, p) level.

[d] E_0[G2(MP2)] = E + Δ(QCT) + Δ(MP2) + E(HLC) + ZPE(HF, scaled) and E(HLC) = $-4.81\ n_\beta - 0.19\ n_\alpha$ (in 10^{-3} au; n_α = number of alpha spin valence electrons; n_β = number of beta spin valence electrons).

[e] E_0[G2(ZPE = MP2)] = E + Δ(QCI) + E(HLC) + $\Delta(+)$ + Δ(2df) + Δ + ZPE(MP2, scaled) and E(HLC) = $-5.13\ n_\beta - 0.19\ n_\alpha$.

Table 2
Comparison of computed barrier heights ($E_0^{\ddagger}$) [a] for the reactions of H with fluoromethanes

	Reactants				
	$CH_4 + H$	$CH_3F + H$	$CH_2F_2 + H$	$CHF_3 + H$	$CF_4 + H$
H-abstraction:	(1h)	(2h)	(3h)	(4h)	
BAC-MP4	61.0	49.6	47.9	54.1	
G2(MP2)	60.3	52.7	51.6	62.0	
G2(ZPE = MP2)	61.2	53.8	52.6	63.2	
QCISD [18]	61.9				
QCISD(T) [19]	57.0				
CCSD(T) [20]	55.8				
PMP4SDTQ [21]	59.4				
POL-CI [22]	65.1				
expt. [23]	62.7				
F-abstraction:		(2f)	(3f)	(4f)	(5f)
BAC-MP4		130.9	149.7	167.2	174.1
G2(MP2)		128.5	154.2	177.1	190.3
G2(ZPE = MP2)		130.9	156.7	179.2	191.9
substitution:		(2s)	(3s)	(4s)	(5s)
BAC-MP4		163.0	216.3	267.3	269.5
G2(MP2)		131.7	191.2	257.6	279.8
G2(ZPE-MP2)		132.2	192.6	261.2	279.8

[a] Energies in kJ mol^{-1} relative to reagents including ZPE, i.e. relative enthalpies at 0 K.

initio values, as well as with the value obtained by fitting to experimental data. For abstraction of hydrogen from methane and the fluoromethanes, the barrier does not vary monotonically with the number of C–F bonds, but does correlate with the calculated TS geometries: the higher barriers are for TSs with longer breaking C–H bonds and shorter forming H–H bonds (Fig. 1). The Evans–Polanyi plot shown in Fig. 2 indicates that knowledge of the reaction enthalpy has predictive power for the barrier to H-abstraction.

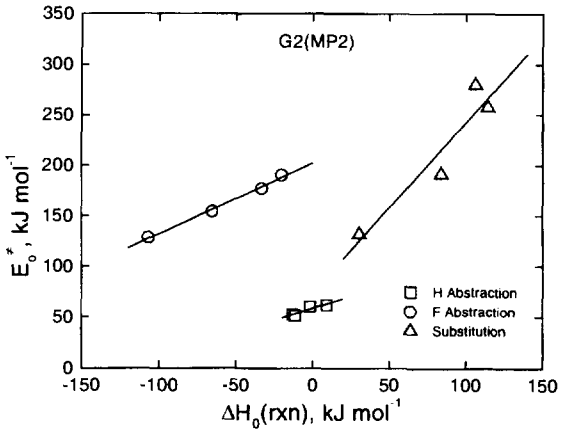

Fig. 2. Calculated G2(MP2) Evans–Polanyi plot for H + fluoromethane reactions (squares = H abstraction; circles = F abstraction; triangles = F substitution).

The barriers to F-abstraction increase along the series from CH_3F to CF_4. There is a good correlation between the calculated $E_0^{\ddagger}$ and ΔH_0 values (see Fig. 2). However, there is only a weak correlation between the C–F and H–F bond distances in the transition states (Fig. 1) and the barriers to abstraction. Because the barriers to abstraction of H atoms are significantly lower than for F-atom abstraction (Table 2) the former channel is expected to dominate under all conditions.

Transition states for substitution reactions involving CH_3F and CH_2F_2 exhibit simple structures where H attacks opposite to the departing F atom (see Fig. 1). For CHF_3 the Hartree–Fock transition state geometry is similar, but the MP2 geometry has the incoming H atom displacing a neighboring F atom. For CF_4 this new transition state geometry is found

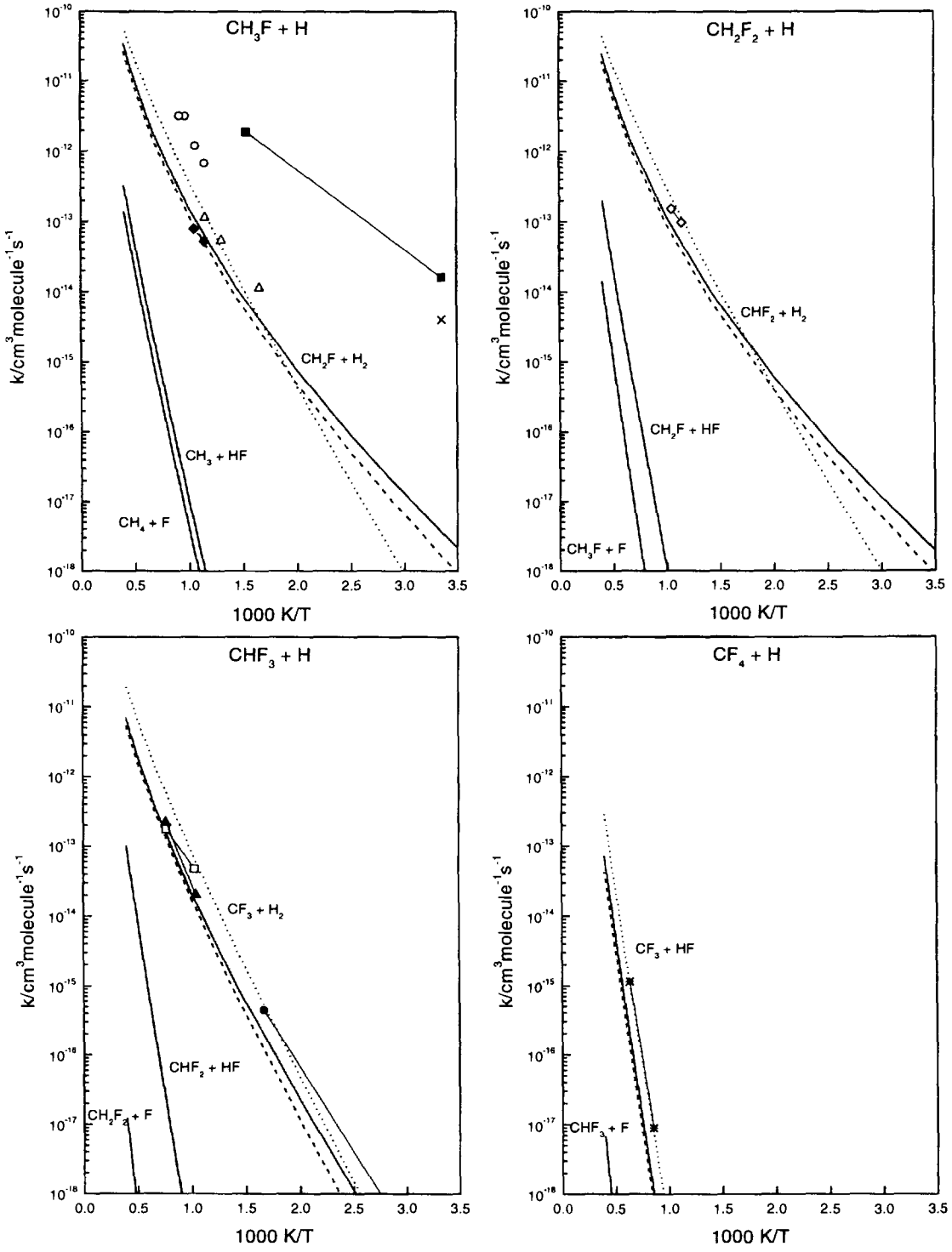
CH3F + H
CH2F + H2
CH3 + HF
CH4 + F
CH2F2 + H
CHF2 + H2
CH2F + HF
CH3F + F
CHF3 + H
CF3 + H2
CHF2 + HF
CH2F2 + F
CF4 + H
CF3 + HF
CHF3 + F
k/cm3molecule-1s-1
1000 K/T

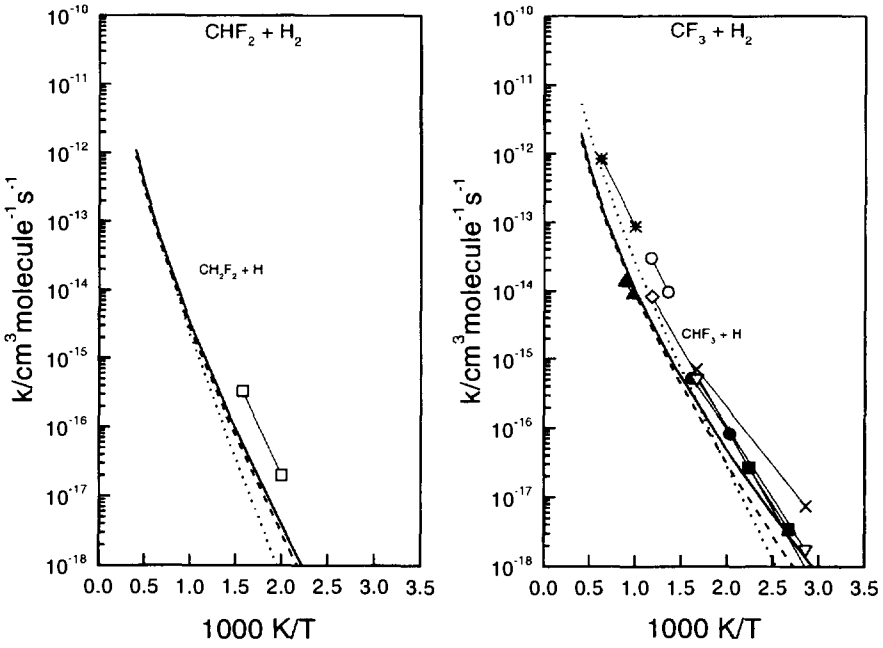

Fig. 4. Comparison of calculated Arrhenius plots for the reverse reaction of H with CH_2F_2 and CHF_3 with experiment. Computed rates are shown as dotted lines for BAC-MP4, solid lines for G2(MP2) and dashed lines for G2(ZPE = MP2). Experimentally determined rates are shown as open squares [25]; closed squares [26]; open circles [27]; filled triangles [28]; crosses [29]; open diamonds [30]; closed circles [31]; inverted open triangles [32]; stars [33].

at both HF and MP2 levels. The new geometry may reflect attraction between the departing F atom and the incoming H atom, which will become more acidic as the extent of fluorine substitution on carbon increases along the series. The non-reacting portions of the TSs assume a geometry akin to the most stable radical geometries, i.e. planar sp^2 for the CH_3 group and pyramidal sp^3 for the CF_3 group. This shift in structure along the series from CH_3F to CF_4 may imply significant differences in the substitution dynamics, but the high barriers mean this pathway will only be important for reactions of translationally hot H atoms.

The G2(MP2) and BAC-MP4 potential energy surfaces for reactions (1)–(5) and possible product channels were employed to calculate the rate constants as outlined in Section 2. The computed Arrhenius plots are compared with experimental results cited in the literature. The forward reaction rate constants are compared in Fig. 3 while the reverse rate constants are compared in Fig. 4 (for $CH_2F_2 + H$ and $CHF_3 + H$). Rate constants based on the G2(ZPE = MP2) energies are also displayed for each major channel.

Since the minor F-abstraction and substitution channels are predicted to have small rate constants, the total rate constant for $H + CH_3F$ is $k_2 = k_{2h} + k_{2f} + k_{2s} \approx k_{2h}$. It may be seen that there is agreement between theory and the earlier recommendation (600–1000 K, factor of 5 error limits) within the experimental uncertainty. If the entire difference between theory and experiment is assigned to the ab

Fig. 3. Comparison of calculated Arrhenius plots for the forward reaction of H with CH_3F, CH_2F_2, CHF_3 and CF_4 with experiment. Computed rates are shown as dotted lines for BAC-MP4, solid lines for G2(MP2) and dashed lines for G2(ZPE = MP2). Experimentally determined rates are shown as open circles (Hart and Grunfelder [7]); open triangles (Westenberg and deHaas [7]); filled squares (Aders et al. [7]); crosses [24]; open squares (Skinner and Ringrose [7]); filled and open diamonds (Parsamyan and Nalbandyan [7]); filled circles (Amphlett and Whittle [7]); filled triangles [3]; and stars (Kochubei and Moin [7]).

initio $E_0^{\ddagger}$ for the reaction, then this corresponds to a computational error of only 4 kJ mol^{-1} (at 800 K). The review by Baulch et al. [7] suggested the dominant channel to be F-atom abstraction, but the rate constant recommendation is based largely on the data set of Westenberg and deHaas [7] who carried out experiments where the disappearance of CHF_3 was monitored in the presence of a large excess of H, so that knowledge of the products was not necessary for determination of the total rate constant.

For reaction (3), $H + CH_2F_2$, H-abstraction is again predicted to be more favorable (see Fig. 3). The computed rate constants compare well (within a factor of 2) with the measurements by Parsamyan and Nalbandyan [7] who studied the ignition limits of CH_2F_2 and derived k_3 in combination with rate constants for $CH_2F + O_2$, although they had assumed F-abstraction to be the main pathway. The rates for the reverse reaction, $CHF_2 + H_2 \rightarrow H + CH_2F_2$, have been measured by Prichard and Perona [25] relative to the rate of recombination of CHF_2 radicals in the 500–635 K temperature range. At 568 K the computed G2(MP2) rate differs by a factor of 6 from experiment.

In Fig. 3 there is a comparison of the forward reaction rate for $H + CHF_3$ with experiment. The rates reported by Amphlett and Whittle [7] (range: 350–600 K) were derived through consideration of the reverse rate constant and the equilibrium constant for $CF_3 + H_2 \rightarrow CHF_3 + H$. Skinner and Ringrose [7] obtained the rates (range: 960–1300 K) by modeling the induction time of shock heated $H_2/O_2/CF_3Br$ mixtures. Richter et al. [3,4] obtained the rates from measurements (range: 960–1300 K) in premixed $H_2/O_2/Ar/CHF_3$ flames. The calculated rates deviate from these experiments by rms factors in the range 0.4 to 0.7 and are closest to the measurements of Richter et al. [3,4]. For the reverse reaction (i.e. $CF_3 + H_2 \rightarrow CHF_3 + H$) the calculated rate constant falls between several reported determinations [26–33], with rms factors in the range 0.1 to 1.3. Close agreement is found with the experimental data of Kibby and Weston [30] (within a factor of 1.3) and Ayscough and Polanyi [26] (within a factor of 0.7).

For $H + CF_4$, the barrier to F-substitution is very high so that F-abstraction is the only accessible channel. The calculated k_{5f} for this slow process is of the same order of magnitude as the measurements by Kochubei and Moin (Fig. 3) [7] who analyzed heated mixtures of CF_4 and H_2, but the measurements imply that the energy of the TS for reaction

Table 3
Summary of TST rate expressions [a] in the form $k = AT^n \exp(-B/T)$ cm^3 $molecule^{-1}$ s^{-1}

Reaction	BAC-MP4			G2(MP2)			G2(ZPE = MP2)		
	A	*n*	*B*	*A*	*n*	*B*	*A*	*n*	*B*
(1h)	1.28e − 16	1.97	6678	1.78e − 23	3.78	3700	9.92e − 21	2.99	4729
(2h)	1.08e − 16	1.96	5394	9.25e − 26	4.40	2279	5.28e − 25	4.17	2631
(2f)	2.87e − 16	1.77	15580	2.06e − 17	1.97	14377	1.27e − 18	2.24	13574
(2s)	4.68e − 16	1.61	19293	5.07e − 17	1.77	14808	8.05e − 17	1.69	14787
(3h)	6.82e − 17	1.98	5249	7.50e − 26	4.39	2218	3.45e − 25	4.18	2538
(3h)(rev)	9.52e − 21	2.69	6210	6.42e − 24	3.53	4315	1.69e − 23	3.39	4502
(3f)	8.14c − 16	1.73	17834	3.03e − 17	2.01	17253	3.10e − 17	1.93	17131
(3s)	8.09e − 24	1.61	25669	1.27e − 16	1.72	21936	1.76e − 16	1.62	22068
(4h)	3.42e − 17	2.01	6391	1.44e − 22	3.38	4514	3.83e − 20	2.68	5469
(4h)(rev)	2.04e − 20	2.74	4916	1.62e − 26	4.27	2368	2.42e − 24	3.64	3138
(4f)	2.23e − 15	1.65	19943	2.60e − 16	1.80	20252	4.79e − 17	1.92	19766
(4s)	7.17e − 16	1.60	31663	2.16e − 18	1.74 [b]	29658	3.36e − 17	1.56 [b]	30424
(5f)	5.11e − 15	1.58	20773	4.83e − 16	1.76	21818	1.00e − 16	1.86	21333
(5s)	1.52e − 15	1.45	31990	1.33e − 17	1.58 [b]	32606	2.45e − 17	1.56 [b]	32696

[a] Obtained by fitting the coupling rate constants at 2500, 2000, 1500, 700, 500, 400, 350 and 298 K. Computed rate constants less than 10^{-19} cm^3 $molecule^{-1}$ s^{-1} were excluded from the fit.

[b] Calculated rate constant at 2250 K was included in order to obtain the rate expression since the rates below 2000 K were smaller than 10^{-19} cm^3 $molecule^{-1}$ s^{-1}.

(5f) has been overestimated by about 22.5 kJ mol^{-1} at the G2(MP2) level. A recent investigation [34] for the entire series of chlorofluoromethanes ($CH_xF_yCl_{4-x-y}$) has determined a BAC for the G2(MP2) method of -8.0 ± 0.4 kJ mol^{-1} per C–F bond. Even if this entire correction were applied to the TS energy (likely an overestimate because the C–F bond is partially broken) a significant difference remains. Thus a confirmation of the measured k_{5f} by a different technique is highly desirable. CF_4 is the calibration molecule for the BAC-MP4 bond additivity correction and we note that this method performs better for this reaction. CF_4 is seen to be several orders of magnitude less reactive than the other fluoromethanes towards atomic hydrogen, because it does not contain labile C–H bonds. The high C–F bond strength also makes unimolecular dissociation unfavorable under combustion conditions. Thus CF_4 is essentially inert in a flame and the flame suppressant activity of CF_4 is largely physical. By contrast, the other fluoromethanes react quickly with H atoms to yield F-containing radicals that undergo further chemistry. This allows the possibility of *chemical* flame suppression by CH_3F, CH_2F_2 and CHF_3.

The rate constants obtained by least-squares fitting to TST calculations at selected temperatures in the range 298–2500 K are summarized in Table 3 in a standard format $k = AT^n \exp(-B/T)$ suitable for combustion models. Note that the individual A, n and B parameters do not have separate physical meanings. Should more accurate kinetic measurements be made in the future, even if only at a single temperature, the rate constant expressions can accommodate this new information simply through adjustment of the B parameter.

A simple parameter which characterizes the quality of agreement between calculation and experiment is $\Delta(\log k)$, the rms difference between $\log(k_{calc})$ and $\log(k_{expt})$. The computed $\Delta(\log k)$ for the G2(MP2) method are 0.5, 0.2, 0.3 and 0.3, for the hydrogen abstraction reaction of CH_4, CH_3F (using recommendations of Baulch et al. [7]), CH_2F_2 and CHF_3, respectively. This indicates that the calculated results are within a factor of ≈ 3 of experiment, which is similar to the deviation between multiple sets of measurements for the same reaction (such as reactions (2h) and (4h)). An exception is the G2(MP2) value for reaction (5f) which has been discussed above. BAC-MP4 calculations yield similar overall agreement with experiment.

4. Conclusions

The ab initio PESs suggest that, contrary to some earlier assumptions, H atoms react predominantly with the C–H bonds in fluoromethanes and that the major product channel is H_2 production. F-atom abstraction is unfavorable kinetically, even though HF formation is the most exothermic pathway. Transition state theory based on BAC-MP4 and Gaussian-2 data gives good accord with experimental rate constants for $H + CH_3F$, CH_2F_2 and CHF_3. Slow F-atom abstraction is the only plausible pathway for H-atom attack on CF_4. Therefore CF_4 is quite unreactive in a flame and acts mainly as a physical flame suppressant. By contrast, the other fluoromethanes react faster with H atoms, so that CH_3F, CH_2F_2 and CHF_3 may participate chemically as well as physically in flame suppression.

Acknowledgement

This work was supported by the Air Force Office of Scientific Research (AFOSR). The authors acknowledge the Materials Directorate and Wright Laboratory for providing the computational and other resources for this work. PM acknowledges support by the AFOSR Summer Faculty Research Program and the Welch Foundation (grant B-1174).

References

[1] C.K. Westbrook, Combust. Sci. Tech. 34 (1983) 201.
[2] F. Battin-Leclerc, G.M. Côme and F. Baronnet, Comb. Flame 99 (1994) 644.
[3] H. Richter, J. Vandooren and P.J. van Tiggelen, 25th Symp. (Int.) Combust. (The Combustion Institute, Pittsburgh, 1994) p. 825.
[4] H. Richter, J. Vandooren and P.J. van Tiggelen, J. Chim. Phys. 91 (1994) 1748.
[5] P.R. Westmoreland, D.R.F. Burgess Jr., W. Tsang and M.R. Zachariah, 25th Symp. (Int.) Combust. (The Combustion Institute, Pittsburgh, 1994) p. 1505.
[6] G.T. Linteris, in: Halon replacements: technology and science, ACS Symposium Series 611, eds. A.W. Miziolek and W. Tsang (ACS, 1995) pp. 260–274.

[7] D.L. Baulch, J. Duxbury, S.J. Grant and D.C. Montague, Evaluated kinetic data for high temperature reactions, Vol. 4. Homogeneous gas phase reactions of halogen- and cyanide-containing species, J. Phys. Chem. Ref. Data 10, Suppl. 1 (1981), and references therein.
[8] M.W. Chase Jr., C.A. Davies, J.R. Downey Jr., D.J. Frurip, R.A. McDonald and A.N. Syverud, JANAF Thermochemical Tables, 3rd Ed., J. Phys. Chem. Ref. Data 14, Suppl. 1 (1985).
[9] D.F. McMillen and D.M. Golden, Ann. Rev. Phys. Chem. 33 (1982) 493.
[10] L.A. Curtiss, K. Raghavachari and J.A. Pople, J. Chem. Phys. 103 (1995) 4192, and references therein.
[11] C.F. Melius, Thermochemistry of hydrocarbon intermediates in combustion. Applications of the BAC-MP4 method (Springer, Berlin, 1990).
[12] M.J. Frisch, G.W. Trucks, V. Head-Gordon, P.M.W. Gill, M.W. Wong, J.B. Foresman, B.G. Johnson, H.B. Schlegel, M.A. Robb, E.S. Replogle, V. Gomperts, J.L. Andres, K. Raghavachari, J.S. Binkley, V. Gonzalez, R.L. Martin, D.J. Fox, D.J. DeFrees, J. Baker, J.J.P. Stewart and J.A. Pople, GAUSSIAN 92 (Gaussian Inc., Pittsburgh, 1992).
[13] R. Steckler, W.-P. Hu, Y.-P. Liu, G.C. Lynch, B.C. Garrett, A.D. Isaacson, D.-H. Lu, V.S. Melissas, T.N. Truong, S.N. Rai, G.C. Hancock, J.G. Lauderdale, T. Joseph and D.G. Truhlar, POLYRATE-version 6.5, University of Minnesota, Minneapolis, (1995).
[14] B.C. Garrett, D.G. Truhlar, R.S. Grev and A.W. Magnuson, J. Phys. Chem. 84 (1980) 1730; 87 (1983) 4454 (E).
[15] R.J. Berry, D.R.F. Burgess Jr., M.R. Nyden, M.R. Zachariah and M. Schwartz, J. Phys. Chem. 99 (1995) 17145.
[16] M.R. Zachariah, P.R. Westmoreland, D.R. Burgess Jr., W. Tsang and C.F. Melius, J. Phys. Chem. 100 (1996) 8737.
[17] R.J. Berry and M. Schwartz, to be submitted for publication.
[18] T.N. Truong, J. Chem. Phys. 100 (1994) 8014.
[19] K.D. Dobbs and D.A. Dixon, J. Phys. Chem. 98 (1994) 5290.
[20] E. Kraka, J. Gauss and D.J. Cremer, J. Chem. Phys. 99 (1993) 5306.
[21] C. Gonzalez, J.J.W. McDouall and H.B. Schlegel, J. Phys. Chem. 94 (1990) 7467.
[22] S.P. Walch, J. Chem. Phys. 72 (1980) 4932.
[23] P.-M. Marquaire, A.G. Dastidar, K.C. Manthorne and P.D. Pacey, Can. J. Chem. 72 (1994) 600.
[24] W.E. Jones and J.L. Ma, Can. J. Chem. 64 (1986) 2192.
[25] G.O. Pritchard and M.J. Perona, Int. J. Chem. Kinet. 1 (1969) 509.
[26] P.B. Ayscough and J.C. Polanyi, Trans. Faraday Soc. 52 (1956) 960.
[27] M.B. Fagarash, F.B. Moin and V.I. Ocheret'ko, Kinetika kataliz 9 (1968) 92 [English transl. Kinet. Catal. 9 (1968) 762].
[28] T. Berces, F. Marta and I. Szilagyi, J. Chem. Soc. Faraday Trans. I 68 (1972) 867.
[29] N.L. Arthur, K.F. Donchi and J.A. McDonell, J. Chem. Soc. Faraday Trans. I 71 (1975) 2431.
[30] C.L. Kibby and R.E. Weston Jr., J. Chem. Phys. 49 (1968) 4825.
[31] G.O. Pritchard, H.O. Pritchard, H.I. Schiff and A.F. Trotman-Dickenson, Trans. Faraday Soc. 52 (1956) 848.
[32] N.L. Arthur and T.N. Bell, Rev. Chem. Intermed. 2 (1978) 37.
[33] Y. Hidaka, T. Nakamura, H. Kawano and T. Koike, Int. J. Chem. Kinet. 25 (1993) 983.
[34] R.J. Berry, D.R.F. Burgess Jr., M.R. Nyden, M.R. Zachariah, C.F. Melius and M. Schwartz, J. Phys. Chem. 100 (1996) 7405.